

# The crystal structures of grossular and spessartine between 100 and 600 K and the crystal chemistry of grossular-spessartine solid solutions

UTA RODEHORST,<sup>1,\*</sup> CHARLES A. GEIGER,<sup>1</sup> AND THOMAS ARMBRUSTER<sup>2</sup>

<sup>1</sup>Institut für Geowissenschaften, Christian-Albrechts-Universität zu Kiel, Olshausenstr. 40, D-24098 Kiel, Germany

<sup>2</sup>Laboratorium für chemische und mineralogische Kristallographie, Universität Bern, Freiestrasse 3, CH-3012 Bern, Switzerland

## ABSTRACT

Spessartine ( $\text{Mn}_3\text{Al}_2\text{Si}_3\text{O}_{12}$ )-grossular ( $\text{Ca}_3\text{Al}_2\text{Si}_3\text{O}_{12}$ ) solid solutions were synthesized at high pressures and temperatures. Compositionally homogeneous garnets are obtained by crystallizing solid-solution glasses prepared from oxides. The unit-cell parameter,  $a$ , for the different solid solutions was determined by X-ray powder diffraction methods and the results give positive deviations from ideal volumes of mixing that can be described with a symmetric mixing model with  $W^v = 0.80$  ( $\pm 0.04$ )  $\text{cm}^3/\text{mol}$ . The degree of non-ideality is a function of the difference in size between the  $\text{Ca}^{2+}$  and  $\text{Mn}^{2+}$  cations and is consistent with the range of those observed for the other aluminosilicate garnet binary joins. The crystal structures of synthetic grossular and spessartine were collected at 50 K intervals between 103 K and 498/648 K using single-crystal X-ray diffraction methods. The rotation of the rigid  $\text{SiO}_4$  tetrahedra changes slightly by  $0.3(1)^\circ$  for grossular and  $0.2(1)^\circ$  for spessartine between 103 and 648 K. The volume expansions of the polyhedra were calculated and their distortions in grossular and spessartine were analyzed as a function of temperature. The linear thermal expansion coefficients of the Al-O and two X-O bond were also calculated for almandine, pyrope, grossular, and spessartine. The thermal expansion of spessartine is similar to that of grossular. In terms of polyhedral distortion and bond-valence values, spessartine has the most ideal structure of the aluminosilicate garnets. This could explain its large  $P$ - $T$  stability field and the ease of synthesis at low pressures.

## INTRODUCTION

Grossular-spessartine garnets are found in nature, but they are restricted to certain petrologic environments. They occur primarily in skarn or metamorphosed sediments of the appropriate bulk composition (Shimazaki 1977). Grossular and spessartine are, of course, important components in solid-solution garnets of metapelites, amphibolites, and granulites. From a crystal-chemical and thermodynamic standpoint, the binary grossular-spessartine solid solution is important for understanding the properties of the silicate garnets as a whole. Spessartine belongs to the pyralspite series and grossular to the ugrandite series of the silicate garnets, yet the two form a continuous solid solution that can be synthesized at moderately low pressures (Ito and Frondel 1968; Hsu 1980). Almandine-grossular and pyrope-grossular solid solutions, in comparison, can only be synthesized at high pressures.

There are a number of reasons that make a study of spessartine-grossular garnets interesting and necessary. First, from an energetic and structural point of view, it is necessary to understand why the solid solution is complete at low pres-

ures and why spessartine can be readily synthesized at 1 atm (Snow 1943). Second, it needs to be clarified if this join has ideal volumes of mixing (Berman 1990; Koziol 1990), because most of the other aluminosilicate garnet joins show measurable nonideality (Geiger and Feenstra 1997; Geiger 1999, 2000).

It also needs to be clarified why spessartine appears to show a relatively large thermal expansion in the temperature range from 200 to 600 K compared to the other silicate garnets (Skinner 1956). From a crystal chemical point of view, grossular needs to be studied as a function of temperature, because Meagher (1975) suggested that its structure changes little with increasing temperature, unlike the other silicate garnets. In addition, it has been proposed that the cations in octahedral and dodecahedral coordination in pyralspite garnets are bonded in an ionic manner, while those of the ugrandites have a higher percentage of covalent bonding (Ungaretti et al. 1995). If true, the grossular-spessartine binary could show potentially interesting structural changes across the join. The stability, thermodynamic, and physical properties of the aluminosilicate garnets are affected by the type of X-site cation present (Geiger 1999), and any potential differences in bonding need to be addressed.

These questions have led us to synthesize garnets along this join and to determine their volumes of mixing. In addition, we undertook a study of the temperature dependence of the grossular and spessartine structures by single-crystal X-ray diffraction at 50 K intervals between 103 and 498/648 K. The data

\* Present address: Department of Earth Sciences, University of Cambridge, Downing Street, Cambridge CB2 3EQ, U.K. E-mail: urod99@esc.cam.ac.uk

allow us to address most of the questions posed above and to investigate more thoroughly the thermodynamic and crystal-chemical properties of the silicate garnets as a whole.

## EXPERIMENTAL PROCEDURES

### Synthesis methods

Spessartine-grossular solid solutions were prepared by two different synthesis methods. In the first, intermediate glasses were prepared by melting finely ground mechanical mixtures of end-member grossular and spessartine glasses in the appropriate proportions. For the second method, intermediate solid solution glasses were prepared by melting stoichiometric mixtures of oxides to the desired composition. The following oxides were used to prepare the glasses: SiO<sub>2</sub> (Alfa, specpure, 99.999%),  $\gamma$ -Al<sub>2</sub>O<sub>3</sub> (Heraeus, 99.99%), CaCO<sub>3</sub> (Alfa, ultrapure, 99.97%), and MnO (Alfa, 99.5%). CaCO<sub>3</sub> was dried at 300 °C for about one day and stored at 110 °C before weighing. SiO<sub>2</sub> and Al<sub>2</sub>O<sub>3</sub> were heated at 1200 °C for about two days before weighing. MnO was treated under an Ar/H<sub>2</sub> stream at 500 °C for about 5 h, until all material reached a green color indicative of MnO, and then was kept in an evacuated desiccator.

For the first synthesis method, end-member glasses of grossular and spessartine composition were prepared by mixing the oxides under distilled water in an agate mortar for about one hour. The grossular oxide mixture was heated in steps of 100° per hour to 800 °C and fired for 12 hours to remove the CO<sub>2</sub>. Then the mixture was melted in a platinum crucible for 30 minutes at 1450 °C. The spessartine mixture was melted in 1 g portions in graphite crucibles at 1250 °C for 30 minutes. The crucibles containing the melts were removed from the oven and the melts were quenched in H<sub>2</sub>O to produce a glass. From the two resulting end-member glasses, about two grams of a mixture to produce the desired solid-solution composition were thoroughly ground in an agate mortar for about 1 h and melted in a graphite crucible between 1250 and 1450 °C. Intermediate garnets were then crystallized from the glass in sealed platinum capsules without H<sub>2</sub>O in an internally heated gas pressure vessel using Argon gas as a pressure medium at 1100 °C and 8 kbar.

For the second method, a total of five grams of an oxide mixture of the appropriate solid-solution garnet composition were thoroughly mixed in an agate mortar under distilled water for about 1 h. The mixture was then heated at a rate of 100°–200°/h to 800 °C and fired between 2 and 12 h to remove CO<sub>2</sub> before melting. This was done under an Ar/H<sub>2</sub> steam to prevent MnO from oxidizing. The oxide mixtures were melted in 1 g portions in covered thick-walled graphite crucibles at temperatures between 1250 °C and 1450 °C, depending on their composition, for 30 to 45 minutes. During the last 2–5 minutes of the procedure, the lid was removed. Garnets were crystallized from the glass in a piston-cylinder device at 1100 °C and 15 kbar without H<sub>2</sub>O in platinum capsules for 4 to 20 h using 3/4 inch talc-glass assemblies.

The resulting polycrystalline synthetic garnets from both methods were found to be optically isotropic, except for composition Gr90Sp10. The garnets were characterized using an automated powder X-ray diffractometer (Siemens D5000) with CuK $\alpha$  radiation. Except for one weak peak belonging to graph-

ite, which appeared in some of the samples prepared by the second method, all diffraction peaks could be assigned to garnet. In the diffraction pattern of the solid-solution Gr90Sp10, 5 to 10% of gehlenite, anorthite and wollastonite were also detected in addition to garnet. The result is independent of the preparation method that was used. Diffraction patterns for the unit-cell refinements were recorded from 15 to 160° 2 $\theta$  using 0.01° 2 $\theta$  increments and 4 seconds counting time per step. Si (NBS 640b) was used as an internal standard. Peak positions were determined with proprietary software (Siemens) by calculating the minimum of the second-order derivative of the peak profile. The *a* lattice parameter was then determined by least-squares methods incorporating 35 to 38 peaks and using the Pulver91 (Weber 1991) program.

The chemical composition and homogeneity of the garnets prepared by the first method and those of the glasses prepared by the second method were determined by a Cameca Camebax electron microprobe. The measurements were made with an accelerating voltage of 15 kV and a beam current of 30 nA. Common oxides and silicates were used as standards. Each analysis represents an average of 10–29 random spot measurements. The garnets prepared by the second method were characterized for chemical composition and homogeneity using EDS analysis on a Cameca SX 50 microprobe using an accelerating voltage of 15 kV. Each analysis represents an average of 50 random spot measurements.

### Temperature-dependent X-ray single-crystal refinements

X-ray data for spessartine were collected at 50 K intervals between 103 and 648 K and grossular between 103 and 498 K. The single crystals were synthesized hydrothermally and are those described in Geiger and Armbruster (1997). One grossular single crystal with a diameter of 80  $\mu$ m was used for all measurements, whereas two different spessartine crystals (diameters of 100 and 60  $\mu$ m) were measured. The first was used for data collection between 103–298 K, and the second was used for the data collection in the range 298–648 K. Low-temperature measurements were performed with a conventional liquid nitrogen-cooling device with a temperature stability of  $\pm$ 5 K. The experiments above 298 K were carried out with a self-constructed hot-air blower with a temperature stability of  $\pm$ 10 K. Intensity data were collected on an Enraf-Nonius CAD4 diffractometer with graphite monochromated MoK $\alpha$  radiation. In order to save counting time, 518 selected reflections showing significant intensity [ $I > 3\sigma(I)$ ] at room temperature in one octant of reciprocal space were collected at each temperature. The upper  $\theta$  limit was 50°. The crystals could be measured with  $\Omega$  scans and a scan angle of 1° + 0.35 tan ( $\theta$ ). Reflection intensities were empirically corrected for absorption by using  $\psi$  scans done at the end of the data collection. Additional information on the experimental conditions is given in Table 1. All data were refined in space group  $Ia\bar{3}d$  with SHELXTL PC 4.1 (Siemens 1993). Because of multiple scattering effects, reflections with  $F_o < 6\sigma(F_o)$  were rejected from the data set as been described in detail by Armbruster et al. (1992). Unit-cell parameters were determined from least-squares refinement of automatically centered reflections (10 12 14 and its symmetric equivalents for grossular and for spessartine below room tem-

**TABLE 1.** Experimental conditions for X-ray single-crystal refinements

	grossular	spessartine(1)	spessartine(2)
Temperature range (K)	103–498	103–298	298–648
Crystal size ( $\mu\text{m}$ )	80	100	60
$\theta$ range ( $^\circ$ )	$<50$	$<50$	$<50$
$h k l$ range	$\leq 24$	$\leq 24$	$\leq 24$
Scan type	$\omega$	$\omega$	$\omega$
Scan angle ( $^\circ$ ) + 0.35 tan ( $\theta$ )	1	1	1
No. of measured reflections	518	518	518
$F_{\text{obs}} > 6\sigma(F_{\text{obs}})$	419	419	419
No. of varied parameters	18	18	18

perature; 8 0 0, 8 8 0, and their symmetric equivalents for spessartine above 298 K). The remaining refinement procedures are similar to those described in Geiger et al. (1992) and Armbruster et al. (1992). The calculation of the polyhedral volumes and distortions was carried out with the program METRIC (Boisen et al. 1993).

## RESULTS

### Grossular-spessartine solid solutions

The garnets prepared by mixing end-member glasses are not compositionally homogeneous, as first indicated by the poor resolution of the  $K\alpha_1$ - $\alpha_2$  doublet around  $60^\circ 2\theta$  in the powder diffraction pattern (Ganguly et al. 1993). Standard deviations in the  $\text{Ca}^{2+}/(\text{Ca}^{2+} + \text{Mn}^{2+})$  ratios, as determined by microprobe analysis, are up to 10 mol%. Most of the unit-cell refinements of such garnets exhibit a larger error in their cell dimension, as compared to the garnets synthesized directly from homogeneous glasses. The measured compositions, the lattice constants, molar volumes and excess molar volumes for the two different sets of Sp-Gr garnets are given in Tables 2 and 3. The listed errors represent  $1\sigma$ .

All compositions show positive deviations from ideality, which is defined by the straight line between Gr and Sp. A

second-order polynomial best fit the volumes of mixing. This is equivalent to a symmetric solution model. Higher order fits were statistically not justified. A weighted least-squares fit leads to the following expression:

$$V(\text{cm}^3/\text{mol}) = 117.95 (1) + 8.15 (7) X_{\text{Gr}} - 0.84 (7) X_{\text{Gr}}^2 \quad (1)$$

where  $X_{\text{Gr}}$  is the mole fraction of Gr in garnet. The excess molar volumes are plotted in Figure 1 and were fit with a symmetric mixing model (Thompson 1967), where  $\Delta V^{\text{xs}} = X_{\text{Sp}} X_{\text{Gr}} W^{\text{V}}$ . The  $W^{\text{V}}$  parameter was determined to be  $0.80 (\pm 0.04) \text{ cm}^3/\text{mol}$  with the data weighted as  $1/\sigma_{\text{Vex}}^2$ . The molar volumes of mixing of the garnets synthesized by mixing end-member glasses are illustrated in Figure 2. Considering their errors, they show ideal behavior (Table 3).

### X-ray single-crystal structural refinements

The number of unique reflections used in the different single-crystal refinements, the lattice parameter,  $a$ , the agreement factor on intensities and the  $R$  values are summarized in Tables 4a and 4b at each temperature for grossular and spessartine. The final atomic coordinates and anisotropic displacement parameters are given in Tables 5a and 5b<sup>1</sup>. The calculated bond lengths and octahedral and dodecahedral volumes and angles are listed in Tables 6a and 6b.

### Thermal behavior of the polyhedra

The  $[\text{Al}_2(\text{SiO}_4)_3]^{6-}$  framework of the aluminosilicate garnets consists of rigid  $\text{SiO}_4$  tetrahedra and  $\text{AlO}_6$  octahedra as demon-

<sup>1</sup>For a copy of Tables 5a, 5b, 6a, and 6b, document item AM-02-004, contact the Business Office of the Mineralogical Society of America (see inside front cover of recent issue) for price information. Deposit items may also be available on the American Mineralogist web site at <http://www.minsocam.org>.

**TABLE 2.** Compositions, unit-cell parameters and molar volumes of spessartine-grossular solid solutions synthesized from solid-solution glasses

Sample	Measured composition $X_{\text{Ca}}$	Error mol% Gr	Unit-cell parameter ( $\text{\AA}$ )	Molar volume ( $\text{cm}^3$ )	Excess molar volume ( $\text{cm}^3$ )
Sp100	0.000(1)	0.08	11.6155(3)	117.968(9)	0.000(13)
Sp90Gr10	0.095(5)	5.00	11.6394(5)	118.698(15)	0.037(17)
Sp85Gr15	0.146(5)	3.37	11.6534(4)	119.127(12)	0.093(15)
Sp80Gr20	0.206(5)	2.32	11.6681(7)	119.578(22)	0.107(23)
Sp75Gr25	0.241(5)	2.08	11.6774(4)	119.864(12)	0.138(14)
Sp60Gr40	0.388(3)	0.86	11.7131(5)	120.967(15)	0.168(17)
Sp50Gr50	0.495(23)	4.66	11.7386(9)	121.759(28)	0.179(29)
Sp40Gr60	0.592(10)	1.74	11.7626(3)	122.507(9)	0.220(13)
Sp25Gr75	0.736(37)	5.04	11.7960(10)	123.554(31)	0.216(33)
Sp10Gr90	0.896(23)	2.58	11.8278(7)	124.555(22)	0.050(25)
Gr100	1.000(1)	0.09	11.8502(4)	125.264(13)	0.000(18)

**TABLE 3.** Compositions, unit-cell parameters and molar volumes of spessartine-grossular solid solutions synthesized from stoichiometric mixtures of end-member glasses

Sample	Measured composition $X_{\text{Ca}}$	Error mol% Gr	Unit-cell parameter ( $\text{\AA}$ )	Molar volume ( $\text{cm}^3$ )	Excess molar volume ( $\text{cm}^3$ )
Sp90Gr10	0.10(1)	10.0	11.6377(10)	118.646(31)	-0.052(32)
Sp75Gr25	0.25(9)	3.4	11.6814(10)	119.987(31)	0.195(32)
Sp60Gr40	0.40(1)	3.3	11.7053(6)	120.725(19)	-0.161(20)
Sp50Gr50	0.50(3)	5.1	11.7350(7)	121.647(22)	0.031(23)
Sp40Gr60	0.61(3)	5.0	11.7594(3)	122.407(9)	-0.012(12)
Sp25Gr75	0.76(1)	1.9	11.7969(10)	123.582(31)	0.069(33)
Sp10Gr90	0.90(2)	2.1	11.8292(8)	124.600(25)	0.065(28)

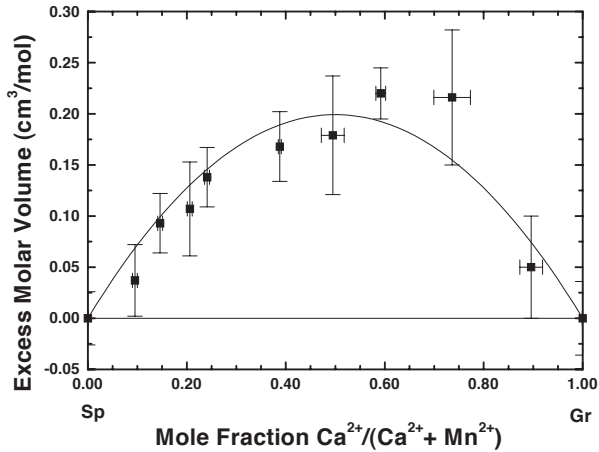


**FIGURE 1.** Excess molar volume plotted vs. composition along the grossular-spessartine join for garnets synthesized from homogeneous glasses. The deviation from ideality can be described with a symmetric solution model. The errors represent  $\pm 2\sigma$  in volume and  $\pm 1\sigma$  in composition.

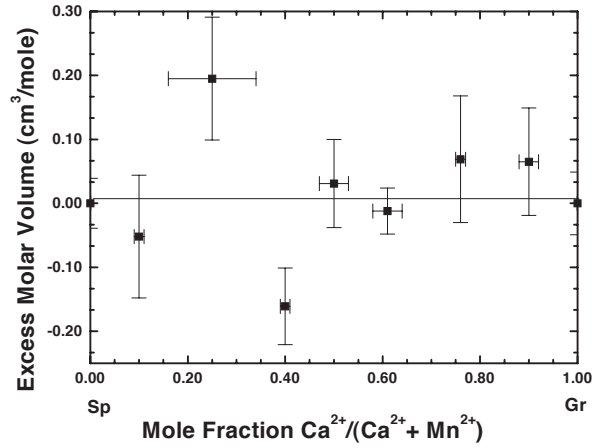


**FIGURE 2.** Excess molar volume plotted vs. composition along the grossular-spessartine join for garnets synthesized from stoichiometric mixtures of end-member glasses. The errors represent  $\pm 3\sigma$  in volume and  $\pm 1\sigma$  in composition.

**TABLE 4A.** Unit-cell dimensions, number of unique reflections with  $F_o > 6\sigma(F_o)$ , and  $R$  values for grossular between 103 and 498 K

$T$ (K)	103	156	205	261	273	298	348	398	448	498
Unit-cell dimension ( $\text{\AA}$ ) ( $\sigma = 0.001 \text{ \AA}$ )	11.840	11.842	11.844	11.847	11.849	11.850	11.853	11.855	11.860	11.867
No. unique reflections $F_o > 6\sigma(F_o)$	322	317	319	298	299	300	280	291	258	266
$R$ (%)	2.26	2.09	2.23	2.07	2.12	2.14	2.21	2.33	2.06	2.09
$R_w$ (%)	5.52	5.46	5.63	5.86	5.47	5.71	5.87	6.46	5.08	5.44
$R_{int}$ (%)	1.18	1.27	1.19	1.26	1.28	1.02	1.05	1.41	1.24	1.27
$R_{\sigma}$ (%)	2.35	2.34	2.29	2.37	2.38	2.3	2.36	2.33	2.36	2.53

**TABLE 4B.** Unit-cell dimensions, number of unique reflections with  $F_o > 6\sigma(F_o)$ , and  $R$  values for spessartine between 103 and 648 K

$T$ (K)	103	156	205	261	273	298	348	398	448	498	548	598	648
Unit-cell dimension ( $\text{\AA}$ ) ( $\sigma = 0.001 \text{ \AA}$ )	11.604	11.608	11.610	11.615	11.615	11.615	11.621	11.622	11.624	11.627	11.632	11.641	11.645
No. unique reflections $F_o > 6\sigma(F_o)$	383	371	375	356	361	262	240	238	248	249	231	224	223
$R$ (%)	2.11	2.14	2.26	2.09	2.26	2.5	2.38	2.39	2.34	2.60	2.56	2.67	2.88
$R_w$ (%)	4.73	5.59	5.77	5.56	5.51	5.26	5.67	5.17	5.54	5.47	5.92	6.46	6.45
$R_{int}$ (%)	1.31	1.16	1.32	1.24	1.26	1.38	1.35	1.50	1.63	1.50	1.82	1.67	1.71
$R_{\sigma}$ (%)	2.01	1.96	1.98	2.02	2.02	3.12	3.6	3.55	3.42	3.37	3.54	3.34	3.55

strated by the nearly temperature independent difference mean-square displacement parameters (dmsdp) along the Si-O and Al-O bonding vectors (Geiger and Armbruster 1997). It should be stressed that this is based on the dmsdp and not on the true lattice dynamic properties. An analysis of the rigid unit modes of the garnet structure shows that tetrahedral deformation must occur following substitution in the X site (Hammonds et al. 1998). This follows from the large number of shared polyhedral edges in the garnet structure, which act to buttress and stiffen it. These internal polyhedral distortions are relatively small, however, and their rigid description can be retained for most descriptions. Both the  $\text{SiO}_4$  and  $\text{AlO}_6$  polyhedra vibrate by external librational and translational motions (e.g., Geiger and Armbruster 1997). Born and Zemann (1964) defined a  $\text{SiO}_4$

tetrahedral angle of rotation, herein noted as  $\alpha_{rot}$ , which decreases with increasing size of the X-site cation in the large dodecahedral site. This angle can be used to describe changes in the tetrahedral-octahedral framework with changing X-site composition. The tetrahedral angle of rotation can be calculated from the atomic coordinates of an oxygen ion, which is located in a general position (i.e.,  $\sin \alpha_{rot} = y/z$ ). The angle,  $\alpha_{rot}$ , decreases very slightly by  $0.2(1)^\circ$  for spessartine and  $0.3(1)^\circ$  for grossular over the temperature range 103 to 648 K (Fig. 3). The values were calculated by linear regression and were extrapolated for grossular above 448 K.

An expansion of the longer X-O4 bond is linked with a rotation of the  $\text{SiO}_4$  tetrahedra to smaller  $\alpha_{rot}$  values. Armbruster et al. (1992) showed that this relationship is valid for a change

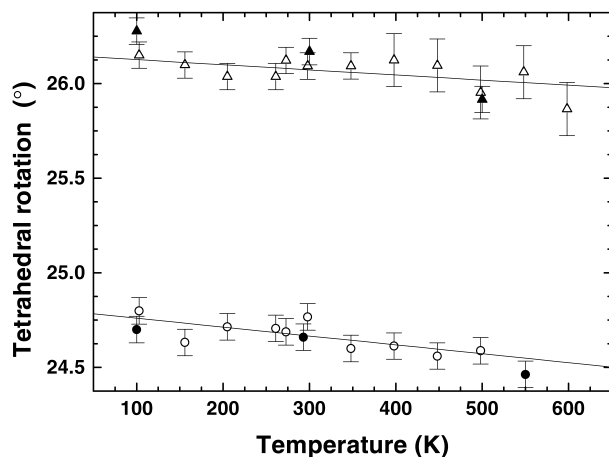


FIGURE 3. The tetrahedral rotation angle of grossular (circles) and spessartine (triangles) vs.  $T$ .

in composition in pyrope-almandine garnets as well as for a change in temperature. The same correlation between  $\alpha_{rot}$  and the X-O4 bond distance can be observed for grossular and spessartine. The degree of tetrahedral rotation is, in addition, correlated with the distortion of the dodecahedron because X-O4 expands more than X-O2 (Armbruster et al. 1992; Armbruster and Geiger 1993; Pavese et al. 1995; Meagher 1975). Distortion of the dodecahedron can also be described simply by the difference  $[\Delta(X-O)]$  between these two crystallographically independent bond lengths (Ungaretti et al. 1995).

The volumes of the  $\text{SiO}_4$  tetrahedron and the  $\text{AlO}_6$  octahedron do not change as a function of temperature within  $3\sigma$ , thus illustrating their rigid nature. The dodecahedron, having the weakest bonds in the garnet structure, is clearly the polyhedron that is most sensitive to changes in temperature (e.g., Armbruster and Geiger 1993; Pavese et al. 1995). Its volume increases as a function of temperature by  $\Delta V_{dod} = 0.31(2) \text{ \AA}^3$  in grossular and by  $\Delta V_{dod} = 0.29(3) \text{ \AA}^3$  in spessartine as calculated by linear regression in the temperature range between 103 and 598 K.

### Thermal behavior of the bonds

The linear thermal expansion coefficient is defined as:

$$\alpha(T) = \frac{1}{l} \left( \frac{dl}{dT} \right) \quad (2)$$

where  $l$  is the bond length. In order to best compare the present results with data from the literature the expansion coefficients were calculated by assuming a linear behavior within the investigated temperature range. Therefore, we fit the data for spessartine, determined at 13 temperatures, and for grossular at 11 temperatures, by linear regression. The linear thermal expansion coefficients for the Al-O and X-O bonds at 298 K are presented in Table 7. They were also calculated using high-precision data for synthetic pyrope, almandine, grossular, and spessartine, which were refined over a similar temperature range of 100–550 K (Armbruster et al. 1992; Armbruster and Geiger 1993; Geiger and Armbruster 1997). The data of Rakai (1975) were used in the calculation of the linear thermal expansion

TABLE 7. Linear thermal expansion coefficients for the Al-O bond and the two crystallographically independent X-O bonds and the mean  $\langle X-O \rangle$  distance for pyrope, almandine, spessartine and grossular

Bond	$\alpha, [10^{-6} \text{ K}^{-1}] = 1/l_{298} (dl/dT)$				Reference
	pyrope	almandine	spessartine	grossular	
Al-O	6.4	6.2	3.5	7	*
	9.6				†
	7			10	‡
			8.4	5	§
X-O2			7		#
	6.2	6.0	6.9	5.7	*
	8.7				†
			10	4.2	‡
X-O4			4.4		§
	15.6	16.3	15.5	13.4	*
	17.5				†
			13.6	11.7	‡
$\langle X-O \rangle$			11.8		#
	10.9	11.1	11.2	9.6	*
	13.1				†
	13			10	‡
		11.6		§	
		8.2	8.0		#

\* Data from Armbruster et al. (1992), Armbruster and Geiger (1993), and Geiger and Armbruster (1997) (100–550K).

† Data from Pavese et al (1995) (30–973K).

‡ Data from Meagher (1975) (298–1023K).

§ Data from Rakai (1975) (303–973K).

# Data from this work (103–498/648K).

coefficients of spessartine. Table 7 shows the resulting thermal expansion coefficients compared to those obtained by Pavese et al. (1995) and Meagher (1975). The coefficients given by Pavese et al. (1995) are valid for the temperature range between 30–973 K (pyrope, four data points), those of Meagher (1975) between 298–1023 K (pyrope, three data points) and 298–948 K (grossular, three data points), and those of Rakai (1975) between 303–973 K (spessartine, four data points).

Bond valence sums were also calculated for spessartine and grossular at all measured temperatures using the expression given by Brown (1992) and the constants proposed by Brese and O'Keefe (1991). The bond valence sums for pyrope and almandine were calculated from data in Armbruster et al. (1992). The calculations show that, from a bond valence analysis, grossular has the most distorted garnet structure (Armbruster and Geiger 1993), because Ca in the X site is strongly overbonded [2.51 valence units (v.u.) at 298 K] having “not enough space” in the dodecahedral cavity.  $\text{Al}^{3+}$  in the octahedral site (2.83 v.u. at 298 K) is underbonded. With increasing temperature the bond valence sum decreases and the grossular structure becomes more “relaxed”, because  $\text{Ca}^{2+}$  obtains more space within the dodecahedral cavity. Pyrope, almandine, and spessartine show a different behavior from grossular. Their X cations are underbonded (1.72 v.u. for  $\text{Mg}^{2+}$ , 1.79 v.u. for  $\text{Fe}^{2+}$ , and 1.93 v.u. for  $\text{Mn}^{2+}$ ) and a decrease in temperature leads to more underbonding.  $\text{Al}^{3+}$  is slightly overbonded, with values of 3.18 v.u., 3.14 v.u., and 3.05 v.u., respectively, for these garnets at room temperature. From this analysis, the spessartine structure is the most “relaxed” of all the end-member aluminosilicate garnets. The bond valence sums of the  $\text{Mn}^{2+}$  and  $\text{Al}^{3+}$  cations are close to their ideal charges of +2 and +3, respectively.

## Vibrations of the atoms

To illustrate the temperature dependence of the mean-square displacement amplitude (msda) of the cations in grossular and spessartine, the tensor component of the msda X-site cations vibrating in the [110] direction with the largest value was analyzed as a function of temperature (Fig. 4). Assuming that all atomic vibrations have the same frequency, the msda of an atom  $j$ ,  $\langle |u(j)^2| \rangle$  should change linearly as a function of temperature at high temperatures according to the following equation (Dove 1993):

$$\langle |u(j)^2| \rangle = \frac{3k_B T}{m_j \omega^2} \quad (3)$$

where  $k_B$  is Boltzmann's constant and  $m_j$  the mass of the atom  $j$ . A deviation from linear behavior at low temperatures is commonly due to zero point motion or static disorder. In garnet no static disorder of the X-site cations has been found (Armbruster et al. 1992; Armbruster and Geiger 1993; Geiger 1999). The data show that the msda of  $\text{Si}^{4+}$  behaves similarly in grossular and spessartine, as does  $U_{\text{eq}}$  of  $\text{Al}^{3+}$ . ( $U_{\text{eq}}$  was considered in the case of  $\text{Al}^{3+}$  instead of the msda, because the two symmetrically allowed tensor components have similar values describing vibration parallel and perpendicular to the  $\bar{3}$  axis). For the X-site cations, the increase in amplitude of vibration with increasing temperature is greater for  $\text{Mn}^{2+}$  than it is for  $\text{Ca}^{2+}$ , reflecting their different site volumes (Fig. 4).

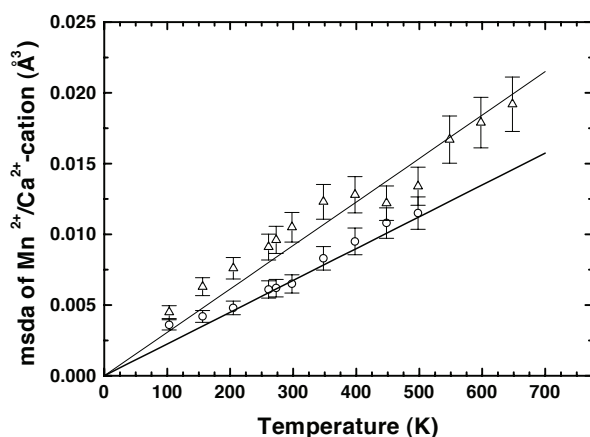


**FIGURE 4.** Mean-square displacement amplitude (msda) of  $\text{Ca}^{2+}$  (circles) and  $\text{Mn}^{2+}$  (triangles) vs.  $T$ . The data were fit by a linear least-squares best fit assuming a mean-square displacement amplitude of  $0 \text{ \AA}^2$  at  $0 \text{ K}$ . This constraint was used in spite of the fact that the grossular data level off below ca.  $200 \text{ K}$ , whereas the spessartine data still decreases. Therefore the fit neglects any zero point motion effects and describes only changes above  $200 \text{ K}$  for grossular. The msda of  $\text{Mn}^{2+}$  in spessartine above  $200 \text{ K}$  increases more than the msda of  $\text{Ca}^{2+}$  in grossular.

## DISCUSSION

### Static structure

**Lattice parameters.** The  $a$  unit-cell dimensions of  $11.6155(3) \text{ \AA}$  and  $11.615(1) \text{ \AA}$  for spessartine determined by powder and single-crystal X-ray diffraction methods at  $298 \text{ K}$ , respectively, are in good agreement (within  $3\sigma$ ) with other determinations (e.g., Hsu 1968; Mottana 1974; Koziol 1990; Geiger and Armbruster 1997). Skinner (1956) proposed a larger value of  $11.621(1) \text{ \AA}$ , which could be due to  $\text{Mn}^{3+}$  at the octahedral position or the presence of  $\text{OH}^-$  (Koziol 1990). The unit-cell dimension of grossular,  $11.8502(4) \text{ \AA}$ , determined by powder X-ray refinement and  $11.850(1) \text{ \AA}$  by single-crystal X-ray diffraction at  $298 \text{ K}$ , agrees well, within  $3\sigma$ , with data from the literature (i.e., Meagher 1975; Hsu 1980; Koziol 1990; Ganguly et al. 1993; Geiger and Armbruster 1997).

**Volumes of mixing.** Of the different aluminosilicate garnet binaries, the volumes of mixing along the pyrope-grossular join show the largest positive deviations from ideality (Geiger 1999). They are asymmetric with the largest deviations toward grossular-rich compositions (Bosenick and Geiger 1997). The almandine-grossular and pyrope-spessartine solid solutions show smaller positive deviations from ideality (Geiger 1999, 2000). The difference in size between the  $\text{Mn}^{2+}$  and  $\text{Ca}^{2+}$  ions, with radii of  $0.96$  and  $1.12 \text{ \AA}$  (Shannon 1976), respectively, in spessartine-grossular garnets is relatively large. Thus non-ideality is to be expected and the magnitude of the measured excess volumes is consistent with simple crystal chemical considerations. Koziol (1990) proposed ideal mixing behavior in her study of the volumes of mixing of grossular-spessartine garnets. However, her garnets were synthesized from mechanical mixtures of end-member glasses and have large compositional inhomogeneities, as do ours prepared using the same method. Such garnets give large errors in the volume. Better compositional homogeneity and more precise X-ray refinements can be obtained by synthesizing garnets from homogeneous solid-solution glasses. Moreover, our measurements give lattice parameters that are more precise and accurate in comparison with previous determinations, because of the improved diffraction methods. There are also no complications relating to the incorporation of  $\text{OH}^-$  in the garnets, because they were synthesized from dry glasses. It is our experience that very precise X-ray measurements are a prerequisite to determine small deviations from ideality (Geiger 1999) and many older measurements on garnet solid solutions do not give an accurate representation of the true mixing behavior. Therefore, we consider the non-ideality illustrated in Figure 1 to be real.

The widths of powder diffraction peaks can be a function of compositional homogeneity, structural state, strain, and grain size in the solid solutions (Bosenick et al. 1999). The FWHM of the 420 reflection is shown for a number of solid solutions prepared by both synthesis methods (Fig. 5). We believe that these measurements do not show major grain size effects, because all our samples were prepared similarly. Generally, the spessartine-grossular garnets synthesized from homogenous glasses have smaller FWHM than those synthesized from mechanical mixtures of end-member glasses. In addition, the

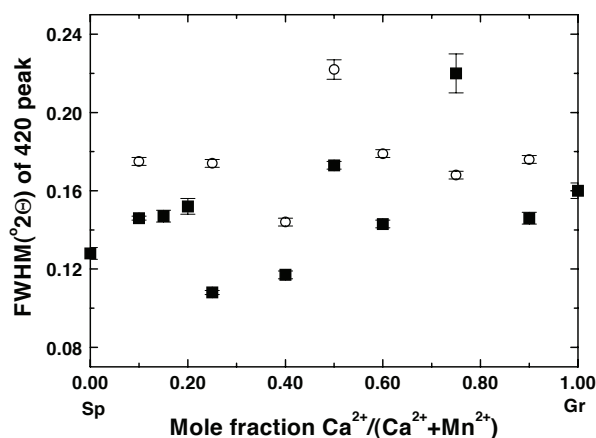


FIGURE 5. Full widths at half maximum (FWHM) of reflection 420 plotted vs. composition. Except for composition Gr75Sp25, the FWHM values are larger for the spessartine-grossular solid solutions prepared from mixtures of end-member glasses (open circles) than those synthesized from homogeneous glasses (filled squares).

spessartine-rich samples have FWHM that are generally narrower than those of grossular-rich compositions.

**Bond valence sums.** Brown (1992) proposed that bond valence sums measure the number of electrons associated with a given bond. The bond valence method is valid for both ionic and covalent bonds, but it does not directly provide information about the kind of bonding. The correlation between Lewis acid strength and electronegativity can be used to estimate the degree of covalency of a bond. Strong Lewis acids, which form strong bonds, will tend to be more covalent in nature. Bonds formed by weak Lewis acids will tend to be more ionic. The Lewis acid strengths of  $\text{Ca}^{2+}$ ,  $\text{Mn}^{2+}$ ,  $\text{Fe}^{2+}$ , and  $\text{Mg}^{2+}$  are 0.274, 0.34, 0.34, and 0.334, respectively (Brown 1992). Therefore,  $\text{Ca}^{2+}$  should, in general, form slightly weaker and more ionic bonds than the other three cations, which have the same Lewis acid strength values. Ungaretti et al. (1995) proposed that  $\text{Ca}^{2+}$  in ugrandite garnets is more covalently bonded in comparison to the X cations in the pyralspites, which they considered to be more ionically bonded. Their proposal is not in agreement with our analysis, but the results of the bond-valence calculations show that the bonding situation in grossular is, indeed, unique for the garnets. The bond valence sum can be thought of counting the number of valence electrons that an atom uses in bonding (Brown 1992) and, because  $\text{Ca}^{2+}$  is strongly overbonded, the electrons of the Ca-O bond probably concentrate near the  $\text{Ca}^{2+}$  cation. This may suggest a more covalent nature, but it can also indicate that the distance between the  $\text{Ca}^{2+}$  and the negatively charged oxygen atoms is short due to structural strain. The bond valence method is not the most appropriate approach to elucidate the type of bonding in garnet, and spectroscopic or precise electron density measurements are needed to analyze the type of bonding in the dodecahedral X site.

#### Temperature dependence and dynamic properties

**Lattice parameters.** The temperature dependence of the lattice parameters was compared to those determined by Skin-

ner (1956) (Table 8), where his polynomials were extrapolated to temperatures down to 100 K. Our  $a$  values of grossular agree well ( $\pm 0.003$  Å) over the whole temperature range with those of Skinner (1956), while our spessartine  $a$  values are all slightly smaller, with larger systematic deviations at higher temperatures (Table 8). Our spessartine data give a slightly smaller thermal expansion that is similar to that of grossular.

**Bond expansion and tetrahedral rotation.** Meagher (1975) found that the  $y$  and  $z$  oxygen coordinates of pyrope shift between 25 °C and 750 °C, whereas those of grossular remain constant. Our results for grossular are not in agreement with these findings. The  $y$  coordinate of the oxygen atoms decreases slightly from  $y(\text{O}) = 0.0478(1)$  at 103 K to  $y(\text{O}) = 0.0473(2)$  at 648 K in spessartine and from  $y(\text{O}) = 0.0456(1)$  at 103 K to  $y(\text{O}) = 0.0451(1)$  at 498 K in grossular. The  $z$  oxygen coordinate seems to increase in both garnets, but a definite change is not observable within the error limits. The  $x$  oxygen coordinate remains constant in both garnets. The linear thermal expansion coefficient of the X-O4 bond for the four different aluminosilicate garnets, pyrope, almandine, spessartine, and grossular decreases as a function of the X-cation size. It has the largest value of  $17.5 \times 10^{-6} \text{ K}^{-1}$  (Pavese et al. 1995) for the Mg-O4 bond in pyrope. The X-O4 bonds in spessartine and grossular have smaller linear thermal expansion coefficients of  $11.8 \times 10^{-6} \text{ K}^{-1}$  and  $11.7 \times 10^{-6} \text{ K}^{-1}$  (this work), respectively. Because the thermal expansion of spessartine and grossular is similar, the values of the linear thermal expansion coefficients of their respective X-O bonds are also similar. Both garnets have smaller values compared to older determinations.

**Polyhedral distortion.** The  $\text{SiO}_4$  tetrahedra in both garnets do not appear to expand or distort with changing temperature, as the bond lengths and bond angles do not change significantly (Tables 6a and 6b). The difference between the two crystallographically independent octahedral angles,  $\Delta(\text{O-Al-O})$ , is related to the octahedral angle variance,  $\text{OAV} = 12(\Delta(\text{O-Al-O})^2)/11$  (Robinson et al. 1971), which Ungaretti et al. (1995) used to describe octahedral distortion. Although the  $\Delta(\text{O-Al-O})$  values (Tables 6a and 6b) show some scatter, the data indicate that octahedral distortion increases in grossular and decreases in spessartine with increasing temperature. The  $\text{AlO}_6$  octahedron in the pyralspites is elongated along the  $\bar{3}$  axis and is flattened in grossular (Ungaretti et al. 1995). With increasing temperature it

TABLE 8. Unit-cell dimensions determined by single-crystal X-ray diffraction between 103 and 498/648 K as compared to those calculated from the polynomials of Skinner (1956)

$T$ (K)	$a$ (spessartine) (Å)			$a$ (grossular) (Å)		
	calculated	measured	difference	calculated	measured	difference
103	11.606	11.604	-0.002	11.838	11.840	0.002
156	11.610	11.608	-0.002	11.841	11.842	0.001
205	11.613	11.610	-0.003	11.844	11.844	0.000
261	11.618	11.615	-0.003	11.848	11.847	-0.001
273	11.619	11.615	-0.004	11.849	11.849	0.000
298	11.621	11.615	-0.006	11.851	11.850	-0.001
348	11.625	11.621	-0.004	11.854	11.853	-0.001
398	11.629	11.622	-0.008	11.858	11.855	-0.003
448	11.634	11.624	-0.010	11.862	11.860	-0.002
498	11.638	11.627	-0.011	11.866	11.867	0.001
548	11.643	11.633	-0.011			
598	11.648	11.642	-0.007			
648	11.654	11.646	-0.009			

becomes less elongated in spessartine, but more flattened and therefore more distorted, in grossular. With respect to distortion of the  $\text{AlO}_6$  octahedron, the substitution of larger X-cations in the pyralspites should be energetically favored (Ungaretti et al. 1995). An increase in temperature has a similar effect as the substitution of a larger X-site cation in pyralspites with regard to octahedral distortion.

The difference in lengths between the two X-O4 and X-O2 bonds,  $\Delta(\text{X-O})$ , describes distortion within the dodecahedron. In the pyralspites, the substitution of larger X cations leads to larger  $\Delta(\text{X-O})$  values and, hence, greater distortion. The same response occurs in spessartine when temperature increases. In the case of the ugrandites, the substitution of larger cations on the X and Y sites results in a decrease of  $\Delta(\text{X-O})$  (Ungaretti et al. 1995). The  $\Delta(\text{X-O})$  values for grossular are larger than in spessartine and they increase with increasing temperature.

In spessartine, the  $\text{AlO}_6$  octahedron is very regular and its structure is the least distorted of the aluminosilicate garnets. All its polyhedra are relatively undistorted and their associated bond valence values are the closest to ideal values at all temperatures. We consider it plausible that these structural factors are, to a large degree, responsible for the large *P-T*-stability of spessartine and spessartine solid solutions and the relative ease in synthesizing them at low pressures.

#### ACKNOWLEDGMENTS

This work was supported by grant Ge 659/2-3 as part of a priority program entitled "Element partitioning in rock-forming minerals" by the "Deutsche Forschungsgemeinschaft." W. Johannes and A. Becker are gratefully acknowledged for the use of the gas pressure vessel at the Institute of Mineralogy at the University of Hannover. We thank B. Mader and D. Ackermann for the microprobe measurements in Kiel and S.J.B. Reed for those in Cambridge.

#### REFERENCES CITED

- Ambruster, T. and Geiger, C.A. (1993) Andradite crystal chemistry, dynamic X-site disorder and structural strain in silicate garnets. *European Journal of Mineralogy*, 5, 59–71.
- Ambruster, T., Geiger, C.A., and Lager, G.A. (1992) Single-crystal X-ray structure study of synthetic pyrope almandine garnets at 100 and 293 K. *American Mineralogist*, 77, 512–521.
- Berman, R.G. (1990) Mixing properties of Ca-Mg-Fe-Mn garnets. *American Mineralogist*, 75, 37–49.
- Breese, N.E. and O'Keefe, M.O. (1991) Bond-valence parameters for solids. *Acta Crystallographica*, B47, 192–197.
- Brown, I.D. (1992) Chemical and Steric Constraints in Inorganic Solids. *Acta Crystallographica*, B48, 553–572.
- Boisen, M.B., Gibbs, G.V., Downs, R.T., and Bartelmehs, K.L. (1993) Program METRIC, Vers. 2.1, University of Texas.
- Born, L. and Zemann, J. (1964) Abstandsberechnungen und gitterenergetische Berechnungen an Granaten. *Contributions to Mineralogy and Petrology*, 10, 2–23.
- Bosenick A. and Geiger, C.A. (1997) Powder X-ray diffraction study of synthetic pyrope-grossular garnets between 20 and 295 K. *Journal of Geophysical Research*, 102, 22649–22657.
- Bosenick A., Geiger, C.A., and Phillips B.L. (1999) Temperature dependent Ca-Mg short-range order in synthetic pyrope-grossular garnets revealed by  $^{29}\text{Si}$  NMR MAS spectroscopy. *American Mineralogist*, 42, 1422–1433.
- Dove, M.T. (1993) Introduction to lattice dynamics, 258 p. Cambridge University Press, U.K.
- Ganguly, J., Cheng, W., and O'Neill, H.St.C. (1993) Syntheses, volume, and structural changes of garnets in the pyrope-grossular join: Implications for stability and mixing properties. *American Mineralogist*, 78, 583–593.
- Geiger, C.A. (1999) Thermodynamics of  $(\text{Fe}^{2+}, \text{Mn}^{2+}, \text{Mg}, \text{Ca})_2\text{Al}_2\text{Si}_3\text{O}_{12}$  garnet: A review and analysis. *Mineralogy and Petrology*, 66, 271–299.
- (2000) Volumes of mixing in aluminosilicate garnets: Solid solution and strain behavior. *American Mineralogist*, 85, 893–897.
- Geiger, C.A. and Ambruster, T. (1997)  $\text{Mn}_3\text{Al}_2\text{Si}_3\text{O}_{12}$  spessartine and  $\text{Ca}_3\text{Al}_2\text{Si}_3\text{O}_{12}$  grossular garnet: Structural dynamic and thermodynamic properties. *American Mineralogist*, 82, 740–747.
- Geiger, C.A. and Feenstra, A. (1997) Molar volumes of mixing of almandine-pyrope and almandine-spessartine garnets and the crystal chemistry and thermodynamic mixing properties of the aluminosilicate garnets. *American Mineralogist*, 82, 571–581.
- Geiger, C.A., Ambruster, T., Lager, G.A., Jiang, K., Lottermoser, W., and Amthauer, G. (1992) A combined temperature dependent  $^{57}\text{Fe}$  Mössbauer and single crystal X-ray diffraction study of synthetic almandine: Evidence for the Gol'danskii-Karyagin effect. *Physics and Chemistry of Minerals*, 19, 121–126.
- Hammonds, K.D., Bosenick, A., Dove, M.T., and Heine, V. (1998) Rigid unit modes in crystal structures with octahedrally coordinated atoms. *American Mineralogist*, 83, 476–479.
- Hsu, L.C. (1968) Selected phase relationships in the system Al-Mn-Fe-Si-O-H: A model for garnet equilibria. *Journal of Petrology*, 9, 40–83.
- (1980) Hydration and phase relations of grossular-spessartine garnets at  $P_{\text{H}_2\text{O}} = 2\text{kb}$ . *Contributions to Mineralogy and Petrology*, 71, 407–415.
- Ito, J. and Frondel, C. (1968) Synthesis of the grossularite-spessartine series. *American Mineralogist*, 53, 1036–1038.
- Kozioł, A.M. (1990) Activity-composition relationships of binary Ca-Fe and Ca-Mn garnets determined by reversed, displaced equilibrium experiments. *American Mineralogist*, 75, 319–327.
- Meagher, E.P. (1975) The crystal structures of pyrope and grossularite at elevated temperatures. *American Mineralogist*, 60, 218–228.
- Mottana, A. (1974) Melting of spessartine at high pressure. *Neues Jahrbuch für Mineralogie, Monatshefte*, 256–271.
- Pavese, A., Artioli, G., and Prencipe, M. (1995) X-ray single-crystal diffraction study of pyrope in the temperature range 30–973 K. *American Mineralogist*, 80, 457–464.
- Rakai, R.J. (1975) Crystal structure of spessartine and andradite at elevated temperatures. Master Thesis, Department of Geology, University of British Columbia.
- Robinson, K. Gibbs, V., and Ribbe, P.H. (1971) Quadratic elongation: a quantitative measure of distortion in coordination polyhedra. *Science*, 172, 567–570.
- Siemens (1993) Shelxtl PC 4.1. Siemens Analytical X-ray Instruments, Madison, Wisconsin.
- Skinner, B.J. (1956) Physical properties of end-members of the garnet group. *American Mineralogist*, 41, 428–436.
- Shannon, R.D. (1976) Revised effective ionic radii and systematic studies of interatomic distances in halides and chalcogenides. *Acta Crystallographica*, A32, 751–767.
- Shimazaki, H. (1977) Grossular-spessartine-almandine garnets from some Japanese scheelite skarns. *Canadian Mineralogist*, 15, 74–80.
- Snow, R.B. (1943) Equilibrium relationships on the liquidus surface in part of the  $\text{MnO-Al}_2\text{O}_3\text{-SiO}_2$  system. *Journal of the American Ceramic Society*, 19, 11.
- Thompson, J.B. Jr. (1967) Thermodynamic properties of simple solutions. In P.H. Abelson, Ed., *Researches in Geochemistry*, 2, 340–361. Wiley, New York.
- Ungaretti, L., Leona, M., Merli, M., and Oberti, R. (1995) Non-ideal solid solution in garnet: crystal-structure evidence and modeling. *European Journal of Mineralogy*, 7, 1299–1312.
- Weber, K. (1991) Pulver 91, Ein Programm zur Auswertung von Pulverdiffraktogrammen, Institut für Mineralogie und Kristallographie, TU-Berlin.

MANUSCRIPT RECEIVED MARCH 19, 2001

MANUSCRIPT ACCEPTED DECEMBER 12, 2001

MANUSCRIPT HANDLED BY ADRIAN J. BREARLEY